AD-A088 278 MATERIALS RESEARCH LABS ASCOT VALE (AUSTRALIA) F/G 20/11
A HIGH-SENSITIVITY POTENTIAL-DROP TECHNIQUE FOR FATIGUE CRACK G--ETC(U)
AUG 79 G CLARK
UNCLASSIFIED MRL-R-755 NL

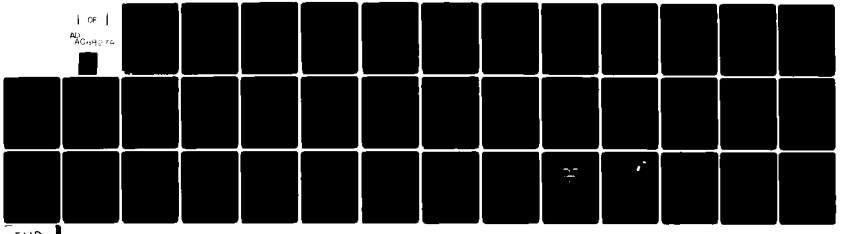

END
DATE FILMED
9-80
DTIC

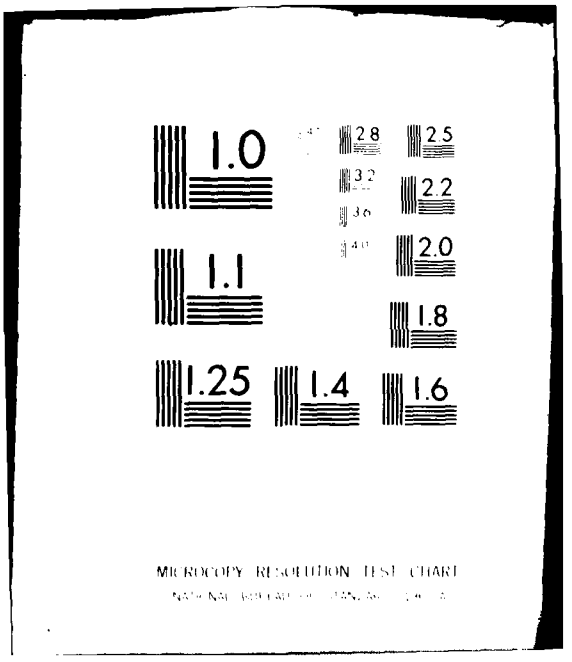
1.0
2.8
2.5
3.2
2.2
3.6
4.0
2.0
1.1
1.8
1.25
1.4
1.6
MICROCOPY RESOLUTION TEST CHART

MRL-R-755

AR-001-837

DEPARTMENT OF DEFENCE

DEFENCE SCIENCE AND TECHNOLOGY ORGANISATION

MATERIALS RESEARCH LABORATORIES

MELBOURNE, VICTORIA

REPORT

MRL-R-755

A HIGH-SENSITIVITY POTENTIAL-DROP TECHNIQUE FOR FATIGUE CRACK GROWTH MEASUREMENTS

Graham Clark

Approved for Public Release

AUGUST 1979

EKRATA

p6 in 3.1(b) "potential" should read
"potential probes".
p15 in line 4 of (7) "etx" should read "enf".
Fig.8 caption:- After "closely," insert "except".

DEPARTMENT OF DEFENCE

MATERIALS RESEARCH LABORATORIES

REPORT

MRL-R-755

A HIGH-SENSITIVITY POTENTIAL-DROP TECHNIQUE FOR FATIGUE CRACK GROWTH MEASUREMENTS

Graham Clark

ABSTRACT

This report describes the design features of a highly sensitive and accurate system for monitoring the growth of fatigue cracks in laboratory specimens of various geometries. The system is based on the potential-drop method which utilises the electrical resistance changes associated with fatigue crack growth through the specimen cross-section to detect crack length increments of a few micrometres. The technique is suitable for automation, and tests may be completed with a minimum amount of operator interference. A computer-based data-processing method is described, and the performance of the system in measuring both absolute crack length and crack growth rate is evaluated.

Approved for Public Release

POSTAL ADDRESS: Chief Superintendent, Materials Research Laboratories
P.O. Box 50, Ascot Vale, Victoria 3032, Australia

DOCUMENT CONTROL DATA SHEET

Security classification of this page: UNCLASSIFIED

1. *DOCUMENT NUMBERS:*
   - a. *AR Number:* AR-001-837
   - b. *Series & Number:* REPORT MRL-R-755
   - c. *Report Number:* MRL-R-755

2. *SECURITY CLASSIFICATION:*
   - a. *Complete document:* UNCLASSIFIED
   - b. *Title in isolation:* UNCLASSIFIED
   - c. *Abstract in isolation:* UNCLASSIFIED

3. *TITLE:*

A HIGH-SENSITIVITY POTENTIAL-DROP TECHNIQUE FOR FATIGUE CRACK GROWTH MEASUREMENTS

4. *PERSONAL AUTHOR(S):*

CLARK, Graham

5. *DOCUMENT DATE:* AUGUST, 1979

6. *TYPE OF REPORT & PERIOD COVERED:*

7. *CORPORATE AUTHOR(S):*

Materials Research Laboratories

8. *REFERENCE NUMBERS:*
   - a. *Task:* DST 77/069
   - b. *Sponsoring Agency:*

9. *COST CODE:* 514720

10. *IMPRINT (Publishing establishment)*

Materials Research Laboratories,
P.O. Box 50, Ascot Vale, Vic.3032

AUGUST, 1979

11. *COMPUTER PROGRAMME(S):*
(Title(s) and language(s)):

12. *RELEASE LIMITATIONS (of the document):*

Approved for Public Release

12-O. *OVERSEAS:* N.O. [ ] P.R. [1] A [ ] B [ ] C [ ] D [ ] E [ ]

13. *ANNOUNCEMENT LIMITATIONS (of the information on this page):*

No Limitation

14. *DESCRIPTORS:*

630 Crack Propagation

15. *COSATI CODES:* 1113

16. *ABSTRACT (if this is security classified, the announcement of this report will be similarly classified):*

This report describes the design features of a highly sensitive and accurate system for monitoring the growth of fatigue cracks in laboratory specimens of various geometries. The system is based on the potential-drop method which utilises the electrical resistance changes associated with fatigue crack growth through the specimen cross-section to detect crack length increments of a few micrometres. The technique is suitable for automation, and tests may be completed with a minimum amount of operator interference. A computer-based data-processing method is described, and the performance of the system in measuring both absolute crack length and crack growth rate is evaluated.

CONTENTS

		Page No.
1.	INTRODUCTION	1
	1.1 Fatigue Cracking	1
	1.2 Fracture Mechanics	2
2.	CRACK LENGTH MONITORING	3
	2.1 Optical Techniques	3
	2.2 Ultrasonic Methods	4
	2.3 Compliance Methods	4
	2.4 Potential Drop Techniques	5
3.	MRL CRACK MONITORING SYSTEM	6
	3.1 General	6
	3.2 Test Procedure	7
4.	P.D. SYSTEM PERFORMANCE	8
	4.1 Changes in Crack Length	8
	4.2 Absolute Crack Length	8
	4.3 Crack Growth Rates	9
5.	CONCLUSION	9
6.	ACKNOWLEDGEMENTS	9
	REFERENCES	10
	APPENDIX A: A REVIEW OF P.D. CRACK MONITORING	12
	APPENDIX B: CURRENT SOURCE AND INPUT LEADS	14
	APPENDIX C: POTENTIAL PROBE SYSTEM	15
	APPENDIX D: AMPLIFICATION AND RECORDING SYSTEM	16
	APPENDIX E: MECHANICAL TESTING SYSTEM MODIFICATIONS	18
	APPENDIX F: POTENTIAL CALIBRATION SYSTEM AND RESULTS	19
	APPENDIX G: COMPUTER PROCESSING OF TEST RESULTS	21
	TABLE I : CALIBRATION EQUATIONS FOR POTENTIAL DROP CRACK MONITORING IN COMPACT TENSION, BEAM AND RING SPECIMEN GEOMETRIES	22

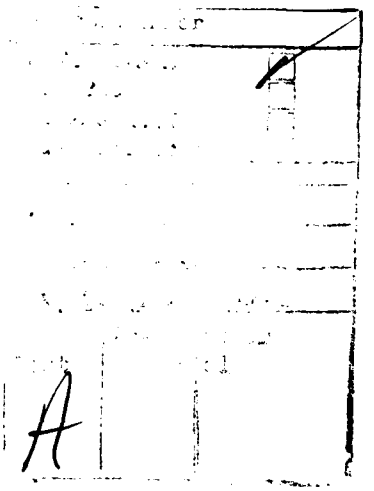

A HIGH-SENSITIVITY POTENTIAL DROP TECHNIQUE FOR FATIGUE CRACK GROWTH MEASUREMENTS

1. INTRODUCTION

1.1 Fatigue Cracking

Fatigue-crack growth is responsible for a majority of failures in engineering components, and may occur in any structure which experiences fluctuating loads. Most fatigue-crack initiation sites are points of high stress concentration, and include surface defects, inclusions, and poor design features such as incorrectly placed notches, holes and changes in cross-section. The stress-concentrating effects of these features may be aggravated by machining marks where cracks develop relatively easily.

Whilst low-strength structural materials have sufficient toughness to enable them to tolerate the presence of long fatigue cracks, a need for lightweight high-performance military equipment has resulted in the increased use of higher strength materials with reduced toughness. In addition, these materials are often required to operate with lower safety factors than were customary and are, in many cases, more likely to show increased crack growth rates in aggressive environments than their low-strength counterparts; the effect of all of these changes has been to reduce the crack length at which fracture instability can occur, and there has been a corresponding increase in interest in techniques which can reduce fatigue failure. These techniques include :-

(i) using processes such as shot-peening, autofrettage and the coldworking of fastener holes to introduce residual compressive stresses which retard the growth of cracks;

(ii) the development of improved non-destructive inspection techniques which can detect defects well before critical length is reached;

(iii) the prediction of crack-growth rates under service conditions so that a defect cannot extend to critical length between inspections.

This report concentrates on (ii) and (iii) which are necessarily closely related.

1.2 Fracture Mechanics

Fracture mechanics procedures are now well established in principle and may be applied to any fatigue cracking problem provided that the following data is available :

(i) The crack length, which may be determined by various methods, including visual, ultrasonic and radiographic inspection.

(ii) The loads experienced by the component. This may be obvious from the original design criteria, or may be obtained by instrumentation of suitable areas of the component with strain-gauges.

(iii) The stress-intensity produced at the crack tip by these loads. For simple cases, this may involve standard solutions, but for more complex geometries, techniques such as finite element analysis may be required.

(iv) The material's fracture toughness, determined using laboratory test procedures which are specified in detail in various standards [1,2].

(v) The fatigue crack growth rate, as a function of crack tip stress-intensity.

The relationship mentioned in item (v) is a property of the material, and usually takes the form shown in Fig. 1, where crack extension per cycle is plotted against the range of stress-intensity (ΔK) experienced at the crack tip, using logarithmic scales. Three regions are evident; region A, approximating closely to a straight line, often extends over several decades of growth rate, and is represented by the expression

$$\frac{da}{dN} = C(\Delta K)^m \qquad (1)$$

At lower stress-intensities (region B), crack growth rates decrease dramatically, reaching zero when ΔK equals the 'threshold' value ΔK_{th}. At high stress-intensities (region C) additional modes of fracture become apparent and crack growth rates increase more rapidly than equation (1) predicts.

In order to estimate the remaining fatigue life of a cracked component, a critical crack length (a_c) is derived from values of fracture toughness (K_c) and service load (σ); in the simple case of an edge-cracked sheet, subjected to uniform tensile loading,

$$K_c = A \sigma \sqrt{\pi a_c} \qquad (2)$$

where A is a factor reflecting the geometry of the sheet and loading system.

If the current crack length (a) is known, then by integrating equation (1)

$$\int_{a}^{a_c} \frac{1}{C(\Delta K)^m} \cdot da = \int dN = N \qquad (3)$$

and it can be seen that in order to determine the remaining life, N, of the component, accurate values of C and, in particular, m are required in equation (1); the accuracy of laboratory procedures for determination of these parameters is therefore of great importance. Unfortunately, while factors such as the material's fracture toughness may be determined to within approximately 10%, laboratory determinations of crack growth rate at any stress-intensity are rarely accurate to better than a factor of two or three; experimental scatter is often seen to cover a full decade of growth rate.

This experimental scatter is usually directly attributable to the fact that small errors in individual crack length measurements in laboratory test specimens lead to much larger errors in crack *extension* as determined from these length measurements. Accordingly, it is necessary to use a highly sensitive and accurate crack length measurement technique. The various methods available for crack length monitoring are described below, together with details of a system, developed at MRL, which permits highly accurate crack growth rate measurements to be made.

2. CRACK LENGTH MONITORING

2.1 Optical Techniques

The majority of fatigue-crack growth rate data is obtained using optical methods. In most cases, a microscope or telescope is used to follow the surface position of the crack tip, and while these methods are capable of great refinement, they suffer from several major drawbacks;

(i) movements of the microscope are subject to mechanical errors,

(ii) subjectivity of the measurement itself,

(iii) the specimen surfaces must be carefully polished,

(iv) crack measurement in aggressive environments may be difficult or impossible.

The major problem, however, arises from the inability of optical methods to monitor crack lengths near the specimen mid-thickness position. The greater elastic constraint in the specimen mid-thickness leads to considerable crack front curvature, with the near-surface crack front trailing that in the centre. This curvature varies with specimen size, as well as with

material properties, and whilst crack extensions of 2 μm may be resolved at the specimen surface [3], it is clearly inappropriate to assume that crack growth characteristics at the surface are representative of crack behaviour in the specimen mid-thickness.

2.2 Ultrasonic Methods

One means of determining the position of a crack front inside the specimen involves the detection of ultrasonic pulses reflected from the crack surfaces [4]. Various arrangements may be used, most of which use a probe which may be moved along the top surface of the specimen, as shown in Fig. 2(a). Movement of the crack front is monitored by moving the probe until the ratio of the amplitudes of the signals reflected from the crack and the lower face of the specimen achieves a particular value (see Fig. 2(b)); the motion of the probe required to maintain this ratio duplicates the movement of crack front. Alternative methods simply monitor the absolute signal returned from the crack tip region.

The accuracy of ultrasonic systems is limited by several factors :

(i) the reflectivity of the crack varies with crack surface roughness, and this can lead to variations in the strength of the reflected signal,

(ii) difficulty in maintaining close contact between the probe and specimen surfaces over long periods,

(iii) the mechanical drive system for the probe is subject to various errors,

(iv) probes are often unsuitable for use in aggressive environments,

(v) difficulty in relating the initial probe position to that of the crack front,

(vi) crack tip plasticity, which affects ultrasonic pulse attenuation and velocity,

(vii) the sensitivity of the system to small increments in crack length is limited.

2.3 Compliance Methods

As the crack length increases, the displacement of the specimen loading points produced by a given load will also increase, and periodic unloading and loading of the specimen will reveal this effect as a change of slope on a load-displacement trace, i.e., a change in specimen compliance. The specimen must be calibrated, and in geometries for which there is no theoretical calibration, this must be done by growing (or cutting) cracks to various depths and measuring the specimen compliance [5,6]. The need to interrupt the fatigue test to determine the crack length and compliance puts a practical limit on the amount of crack length data which may be obtained from one test, and hence on the number of growth rate determinations. The data in reference 5 is of particular interest in that it was obtained from

specimens fatigued in an aggressive aqueous environment (sodium chloride solution) which would normally make measurements with other techniques difficult to obtain.

2.4 Potential Drop Techniques

The electrical potential or potential drop (P.D.) crack monitoring technique involves the measurement of the specimen's electrical resistance, which increases as crack extension gradually reduces the remaining cross-sectional area. The absolute resistance of steel specimens is very low (of the order of 20 μΩ for a compact tension specimen) and the measurement technique usually involves passing a constant direct current through the specimen and monitoring the increasing potential across the cracked section as the crack extends and the resistance increases. However, voltages are very low and currents of 30 to 50A are often necessary in order to improve sensitivity to an acceptable level. Amplification of the voltage signal is usually required in order to permit easy recording of the signal, and the design of the voltage detection and amplification system requires great care to prevent degradation of the signal by electrical noise. Two specimen geometries are illustrated in Fig. 3.

Calibration of the electrical system is necessary, and it is usual to develop a calibration polynomial of the form

$$a/W = Ao + A_1 (V/Vo) + A_2 (V/Vo)^2 + ... A_n (V/Vo)^n \qquad (4)$$

where a, W and V are the crack length, specimen width and voltage parameters shown in Fig. 3, and Vo is the value of V at the beginning of the test (i.e. when $a/W = a_o/W$).

Calibration techniques involve either real or analogue specimens. With real specimens, a "crack" is cut into the specimen, and voltage readings are taken as this crack is extended [7]. However, as disconnection and reconnection of the current leads and potential probes can lead to errors from contact resistance changes, it is often necessary to cut the "crack" with all leads connected to the specimen. This may be difficult, and one means of avoiding the problem is to grow a fatigue crack in the specimen, applying periodic overloads which produce characteristic striations on the fracture surface [8]. At the end of the test, the specimen is broken open, and the crack front position for each voltage reading may be determined by locating the appropriate striation on the fracture surface. This technique, whilst having the clear advantage that calibration and test conditions are identical, is sometimes limited by difficulties in locating the striation marks on the fracture surface. On the other hand, calibration methods which rely on surface measurement of cracks [9,10] are somewhat unsatisfactory as the surface crack length is not representative of the crack length measured in the specimen interior.

Analogue calibration methods use enlarged two-dimensional conducting paper "specimens", in which "cracks" may be cut with great accuracy, and which develop much higher voltages than are encountered in the real specimen.

The P.D. technique has a number of advantages over other methods;

(a) very high sensitivity to changes in crack length may be achieved,

(b) a continuous record of crack length may be acquired,

(c) no operator action is required during the test,

(d) tests may be carried out remotely in an environmental chamber,

(e) an "average" crack length is determined, rather than surface measurements.

The technique does however require high-quality electronic amplification, and great care in design of the voltage probe system. Electrical isolation of the specimen is also necessary.

A brief review of the development of P.D. crack monitoring is given in Appendix A.

3. MRL CRACK MONITORING SYSTEM

3.1 General

The testing facility to which a P.D. crack monitoring system has been added uses a 500 kN load capacity MTS servohydraulic testing machine. The majority of specimens on which fatigue testing is performed are of the CTS geometry (Fig. 3(a)), but a variety of other geometries are occasionally used, including ring specimens (Fig. 3(b)), and P.D. facilities (including calibrations) for these geometries are therefore required.

The major features of the P.D. system, which is shown schematically in Fig. 4, include the following :

(a) A 50 A constant direct current power supply. A detailed description of this unit, and the system of leads and contacts used to feed the current through the specimen, is given in Appendix B.

(b) A system of potential which minimises electrical noise and thermal e.m.f.'s (Appendix C).

(c) An amplification and recording system with extremely low drift and low noise characteristics (Appendix D).

(d) Several modifications were made to the testing frame, primarily for electrical insulation (Appendix E).

(e) Calibrations were performed using conducting paper analogue specimens (Appendix F).

(f) All results were processed using a computer program PDPROG which is described in Appendix G.

The procedure used for a fatigue test varies with specimen type, as a result of variations in current lead and voltage probe positioning. However, that used for the CTS specimen is typical and is detailed below.

3.2 Test Procedure

With a constant range of cyclic loading there is insufficient span in ΔK available with the specimen shown in Fig. 3(a) to obtain enough data for fully characterising the linear region A shown in Fig. 1. It is therefore necessary to make a number of load increases during the test in order to obtain data from a wide enough range of ΔK and growth rate. The use of specimens with shorter initial notches will allow more fatigue crack growth data to be obtained.

The P.D. calibration for the CTS specimen geometry with $a_o/W = 0.3$ is given in Appendix F, and takes the form of a polynomial in $(\Delta V/Vo)$ where $\Delta V = (V-Vo)$. The test procedure involves the following steps :

(a) Current leads and potential probes are attached to the specimen, using the appropriate screw holes, and a current of 50 A passed through the specimen.

(b) A transparent plastic shield is used to protect the specimen from local temperature variations.

(c) The specimen is loaded to the maximum load of the cyclic waveform expected to be required for crack initiation, after which the load is reduced to the mean load of the cycle, and is then held constant. This ensures that potential changes associated with notch plasticity occur before a reading of Vo is taken.

(d) The system is allowed to stabilise for approximately one hour.

(e) A reading of Vo (typically 1.5 mV) is taken.

(f) An offset signal is applied to the amplifier to remove this Vo reading; the system now given ΔV as an output.

(g) Cyclic load is applied. High load levels (typically those giving $\Delta K = 20$ MPa $\sqrt{m}$) are used in order to initiate a fatigue crack as quickly as possible.

(h) The load is reduced when the value of ΔV indicated corresponds to $a/W = 0.32$ with further reductions at 0.34, 0.36 and 0.37, until at $a/W = 0.37$, the crack is growing at the required minimum ΔK for the test (typically $\Delta K = 12$ to 15 MPa $\sqrt{m}$). These steps are extremely important, since it is necessary to use the initial crack growth stage to allow crack front curvature to develop and stabilise, and to ensure that the crack front has passed through the large plastic zone which results from the high initiation loads.

(i) The crack is allowed to grow until sufficient data for part of the log (da/dN) vs. log ΔK plot has been obtained. The load is then increased, usually at crack lengths of a/W = 0.5 and a/W = 0.625.

(j) When the crack length reaches a/W = 0.8, the test is discontinued.

(k) Initial data identifying the specimen, its size and geometry, and Vo is placed in a computer file 'DATA' (see Appendix G).

(l) Corresponding values of ΔV, N (number of cycles) (maximum and minimum loads) throughout the test are used as input in program 'DATA'.

(m) The main program 'PDPROG' is run, and produces plots of *a* vs. *N*, *log(da/dN)* vs. *log (ΔK)*, *log (da/dN)* vs. *a*, and *log (ΔK)* vs. *a*, as well as a printout of all results.

4. P.D. SYSTEM PERFORMANCE

4.1 Changes in Crack Length

Tests on 25 mm thick CT specimens show that changes in potential of 0.5 μV are detectable with ease. This corresponds to an increase in crack length of approximately 20 μm at short crack lengths or 10 μm for longer cracks near the end of a test.

4.2 Absolute Crack Length

The analogue specimen calibration technique used at MRL is entirely two-dimensional, and the current input arrangement used for the real specimen is designed to ensure that the real system approximates closely to a two-dimensional current flow. However, the curvature of the crack front cannot be represented in the two-dimensional calibration, and the P.D. system will therefore provide only a mean crack length.

This effect was investigated using a series of mild steel beam specimens, in which fatigue cracks were grown from 45° V-notches by loading in three-point bending. The P.D. system was connected to the specimen as shown in Fig. 5. Various specimen thickness (B) values were used, and cracks were grown until the P.D. system indicated a crack length near a/W = 0.5. When the specimens were broken open, the crack front profiles could be measured and compared with the final P.D. indication of crack length, and the crack front profile of the thickest specimen (with B = 57 mm) is shown in Fig. 6, together with the P.D. measurement of a/W = 0.509. It is clear that the P.D. system provides a much better estimate of crack length than surface measurement techniques, and in addition, it can be seen that the P.D. crack length estimate is very close to the crack length measurement used in fracture toughness test procedures [1,2], namely, the mean of crack lengths measured at the quarter, mid-thickness and three-quarter thickness positions.

In Fig. 6, the P.D. estimate of crack length lies some 70% of the way between the trailing and leading crack front positions. This figure varies with specimen thickness, as shown in Fig. 7; for all but the thickest specimen, the value lies between 60 and 70%. In the thicker specimens, the straight portion of the crack front is more pronounced than in those in which plane stress conditions extend across a large part of the thickness, and it would therefore be expected that the P.D. system will indicate crack lengths in thick specimens which more closely approach the "leading" part of the crack front. This effect is seen in the thickest (B = 57 mm) specimen described here.

It is clear from the above that estimating the ability of the P.D. technique to determine absolute crack lengths is inherently difficult. However, in specimens which have been fatigue-cracked to give the same P.D. estimate of crack length, the true mid-thickness crack lengths appear to differ by only a small fraction of a millimetre.

4.3 Crack Growth Rates

Figure 8 shows the relationship between *log (da/dN)* and *log* ΔK determined for two specimens from an ESR steel casting. The specimens were machined from adjacent positions and it is clear that the differences between the curves for the two specimens are very small. Over the region of the curve in which local material variations are expected to have minimal effect (the central 'straight line' portion) crack growth rates for the two specimens are within 5%. Only in the high - ΔK 'overload' region do significant differences appear, and this is consistent with normal variations in such factors as inclusion content which would be expected to affect growth rates in this region.

5. CONCLUSION

A potential drop crack monitoring system capable of detecting crack length changes of less than 20 μm has been developed at MRL. Using this system, the crack growth rate and crack tip stress intensity relationship may be determined to a very much higher accuracy than is possible with other crack monitoring techniques.

6. ACKNOWLEDGEMENTS

Invaluable assistance was provided at all stages by Mr. T.V. Rose and by Mr. D. Sadedin in design of the amplification system.

REFERENCES

1. ——. (1975). "Standard Method of Test for Plane Strain Fracture Toughness of Metallic Materials". *ASTM E399-74, ASTM, Philadelphia.*

2. ——. (1977). "Methods for Plane Strain Fracture Toughness (K_{Ic}) Testing". *BS 5447, British Standards Institution.*

3. Ritter, J.C. and Burke, D.J.S. (to be published).

4. Clark, W.G., Jr. (1966). *Westinghouse Research Laboratory Report No. 66-1B4-BTLFR.*

5. Sullivan, A.M. (Dec. 1975). *NRL Report No. 7941, Naval Research Labs., Washington, D.C.*

6. Misawa, T., Ringshall, N. and Knott, J.R. (1976). *Corros. Sci.*, 16, 805.

7. Ritchie, R.O. (Jan. 1972). *Internal Report, Department of Metallurgy, University of Cambridge.*

8. Trost, A. (1944). *Metallwirtsch*, 23, 308.

9. Che-Yu Li and Wei, R.P. (1966). *Materials Research and Standards*, 6, 392.

10. Johnson, H.H. (1965). *ibid*, 5, 442.

11. Gille, G. (1956). *Maschinenschaden*, 29, 123.

12. Barnett, W.J. and Troiano, A.R. (1957). *J. Metals*, 9, 486.

13. Steigerwald, E.A. and Hanna, G.L. (1963). *Proc. Am. Soc. Test. Mater.*, 62, 885.

14. Anctil, A.A., Kula, E.B. and DiCesare, E. (1963). *ibid*, 63, 799.

15. Ritchie, R.O., Garrett, G.G. and Knott, J.F. (1971). *Int. J. Frac. Mech.*, 7, 462.

16. Clark, G. (1975). "Fatigue Crack Growth from Notches". *Ph.D. Thesis, University of Cambridge.*

17. Clark, G. and Knott, J.F. (1975). *J. Mech. Phys. Solids*, 23, 265.

18. Gilbey, D.M. and Pearson, S. (Dec. 1966). *Royal Aircraft Establishment Tech. Report 66402, Farnborough, England.*

19. Jack, A.R. and Price, A.T. (1970). *Int. J. Frac. Mech.*, 6, 401.

20. Jack, A.R. and Yeldham, D.E. (July 1970). *CEGB (Midlands) Report SSD/MID/R/215/70.*

21. McCartney, L.N., Irving, P.E., Symm, G.T., Cooper, P.M. and Kurzfeld, A. (Feb. 1977). *National Physical Laboratory Report DMA(B)3, Department of Industry, England.*

22. Ritchie, R.O. and Bathe, K.J. (1979). *Int. J. Fract.*, 15, 47-55.

23. Ingham, T. and Sumpter, J.D.G. (1978). "Tolerance of Flaws in Pressurised Components". *Paper C93/78, Conference, Inst. Mech. Engrs., London.*

24. Carlsson, A.J. (1962). *Trans. Royal Inst., Stockholm, Sweden, No.189.*

25. Marandet, B. and Sanz, G. (1977). *ASTM STP631, ASTM, Philadelphia, 462-476.*

26. Srawley, J.E. and Brown, W.F. (1964). *ASTM STP381, ASTM, Philadelphia, 113.*

27. Srawley, J.F. and Brown, W.F. (1966). *ASTM STP410, ASTM, Philadelphia.*

28. Unwin, P.N.T. and Smith, G.C. (1969). *J. Inst. Metals*, 97, 299.

29. Davies, J., Cannon, D.F. and Allen, R.J. (1970). *Nature Phys. Sci.*, 225, 1240.

30. Lowes, J.M. and Fearnehough, G.D. (1971). *Eng. Fract. Mech.*, 3, 103-108.

31. Landes, J.D. and Begley, J.A. (May 1976). *Westinghouse Scientific Laboratories, Paper 76-IE7-JINTF-P3.*

32. McIntyre, P. and Priest, A.H. (1971). *BISRA Open Report No. MG/54/71, British Steel Corporation, London.*

33. Bachman, V. and Munz, D. (1979). *Eng. Fract. Mech.*, 11, 61.

34. Clarke, C.K. and Cassatt, G.C. (1977). *ibid*, 9, 675.

35. Unangst, K.D., Shih, T.T. and Wei, R.P. (1977). *ibid*, 9, 725.

APPENDIX A

A REVIEW OF P.D. CRACK MONITORING

The use of electrical resistance changes to monitor crack length damage is not new; Trost in 1944 [8] used this method to detect surface cracks in actual structures, as did Gille in 1956, using currents in excess of 1000 A [11]. In laboratory tests, Barnett and Troiano [12] used a Kelvin bridge to investigate hydrogen embrittlement cracks in notched round specimens, and Steigerwald and Hanna [13] applied similar methods to a cracked sheet geometry.

Anctil [14] produced data relating crack lengths in aluminium foil specimens to changes in resistance, and this data was examined by Johnson [10], who found that there was poor agreement with a theoretical relationship. However, agreement improved substantially when the theoretical relationship was modified to account for the presence of an elliptical starter-notch [9].

It is common practice to use analogue specimens (suitably magnified to give greater accuracy in cutting 'cracks') cut from conducting paper, to produce calibration data relating the potential across the faces of an extending crack to the crack length [15-17]. A constant current (usually d.c.) is passed through the specimen, and the calibration is presented in a form similar to

$$a/W = Ao + A_1 (V/Vo) + A_2 (V/Vo)^2 + \ldots + A_n (V/Vo)^n \qquad (A1)$$

One benefit of using conducting paper specimens is that equipotential lines may be plotted on the paper and used to optimise the position of potential probe leads [16]. This problem has also been studied theoretically by Clark and Knott [17] for specimens containing semi-elliptical and V-notches.

Conformal mapping techniques may be used to analyse the current flow in simple geometries, and this technique has been used by Gilby and Pearson [20], who derived calibration curves for a variety of centre-cracked and edge-cracked geometries; these curves were found to give excellent agreement with experiment [19,20]. Similar techniques were used by Clark and Knott [17] to develop calibrations for cracks growing from semi-circular, semi-elliptical and V-notches. Recently, calibrations have been performed for a simplified form of the compact tension specimen, using integral equation techniques [21] and for beam and CTS geometries using finite element analysis [22].

The use of a.c. potential drop techniques has been described by several authors [23-25], and offers the advantages of high noise rejection and low current consumption. However, as the frequency of the current increases, the 'skin effect' (the concentration of current density in the surface

layers of the specimen) also becomes considerable, and this leads to problems in calibrating the system; clearly, no analogue calibration technique can be used.

Potential drop techniques have been applied to a variety of fracture problems - the detection of crack initiation has been attempted in K_{Ic} tests [26-28], COD tests [29,30] and more recently in J_{Ic} testing [31,23,25]. In addition, hydrogen embrittlement cracks [12], creep cracks [20,32] and fatigue crack closure [34-36] have been studied, and the velocities of running cleavage cracks have been measured [24].

APPENDIX B

CURRENT SOURCE AND INPUT LEADS

The requirements for the source of constant current are :

(a) Current of approximately 50 A, constant to better than 0.05%. In order to limit specimen heating, current densities should be limited to a maximum of 40 A/cm^2 [30].

(b) Low temperature coefficient or a thermally-stabilised environment for the supply.

(c) Voltage capacity of approximately 10 V. For most applications, no more than 2 V should be required, most of which is accounted for by voltage drop in the current leads.

(d) Low resistance current leads and contacts, in order to minimise heating effects and to limit power dissipation.

(e) Electrically floating output, in order to avoid the introduction of stray AC noise signals through an earthing system. If the output is earthed, this must be made the earth for the whole P.D. system.

(f) Rapid warm-up, in order to minimise the time lost in re-stabilising the system after changing specimens. As an alternative, the supply should be operated continuously, by switching in a shunt in place of the specimen during specimen changes.

The source used in the MRL system is a Hewlett-Packard 6259B power supply, with a 50 A, 10 V capacity and drift of less than 0.05%. The supply is connected to the specimen by 150 A capacity welding cable. At the specimen end, the cables are bolted to copper blocks which are used to introduce the current; the design of these blocks varies slightly according to specimen design. For all geometries, however, it is important that the current is introduced uniformly over the specimen thickness, in order that the whole system approximates to the two-dimensional calibration arrangement. In addition, it is essential that any screws used to hold the copper blocks to the surface do not conduct any current themselves, in order to avoid the uncertain electrical contact found in screw threads. The current introduction system for CT specimens is shown in Fig. B1, and that used for ring specimens differs only in that the contact surface is curved to conform to the outer radius of the ring, and in the clamping system; in the ring specimen the blocks are attached by clamps passing through the central hole in the ring.

For beam specimens, current is introduced at the ends of the beam, and within a short distance [16] uniform current conditions are established. Hence, the attachment system is not important, and the current is introduced via screw holes in the ends of the specimen.

APPENDIX C

POTENTIAL PROBE SYSTEM

The probe system used to monitor the voltage across the cracked section of the specimen must detect extremely low voltages with a minimum of noise, and hence must satisfy the following requirements :

(a) Whenever possible, contact between different metals must be avoided. Such contact could lead to thermal potentials which could obscure changes in the signal; for example, the Fe/Cu junction has a thermal efm of 12 μV/°C, which is unacceptable without very careful temperature control [7].

(b) The probes should be thermally isolated from air currents.

(c) The probe leads should be as short as possible, and electrically screened.

(d) The probes should be easy to connect.

The MRL system uses steel wire leads, in order that the necessary Fe/Cu junction may be enclosed in the amplifier case, rather than be exposed on the specimen surface. The location of the probes is determined for each geometry using the equipotential plotting procedure described in Appendix F; each of the probes may be placed at any point on the thickness, as the specimen conforms closely to the two-dimensional analogue arrangement. In some cases [7,16] the probes are offset diagonally across the notch in order to enhance the crack length averaging characteristics of the technique, but this has the disadvantage that thermal gradients in the specimen can produce greater thermal potentials when the probes are widely separated, and in this case it was decided to minimise this effect by locating both probes on the mid-thickness line of the specimen.

For the CTS geometry, connection is made (Fig. B1) by means of screws which clamp a connector (crimped to the end of the probe lead) between the screw head and a PTFE cylinder. These steel screws are located in holes positioned carefully at each side of the notch, and the cylinder of PTFE provides thermal insulation for the contact system and removes the need for nuts, hence simplifying the connection procedure.

Beam specimens use an identical system to that for the CTS geometry, but for the ring specimen geometry (Fig. 3(b)) it is not possible to drill holes for locating the probe leads, and a capacitance discharge welder is used to attach a length of steel probe wire directly to the probe positions. This wire must then be attached mechanically to the probe lead, as it is necessary to isolate the amplification system electrically during discharge welding. The mechanical connection is thermally insulated with heat-shrinkable tubing.

APPENDIX D

AMPLIFICATION AND RECORDING SYSTEM

Very low noise, low drift amplification of 60 dB gain is used to bring the potential across the crack to a suitable level for recording. A circuit diagram is shown in Fig. D1, and the major features of the unit are listed and discussed below.

(a) The amplifier used (Analog Devices 261K) is a non-inverting chopper-stabilised amplifier with a specified noise level of 0.4 μV peak-to-peak, and drift of less than ± 0.5 μV per month. A temperature coefficient of 0.1 μV/°C is low, but significant, and the amplifier and its associated circuitry are mounted inside a diecast box which is packed, inside thermal insulation, inside the outer instrument case. A stabilised 15-0-15 volt power supply is mounted in a similar instrument case above the amplifier, and a thermal screen and air gaps between the cases ensure that convection set up by the upper case draws air at ambient temperatures over the lower (amplifier) case.

(b) As mentioned in Appendix C, the Fe/Cu junctions required in the potential probe leads are located near the amplifier inside the inner case, in order to ensure a temperature-controlled environment and prevent thermal emf's. The junctions themselves consist of two copper blocks with holes into which the steel probe wires are inserted (and locked with copper screws). These blocks are mounted on, and thermally (but not electrically) connected to, another copper block immediately adjacent to the amplifier.

(c) Low thermal emf solder is used for all joints in the low-voltage region of the amplifier, and the resistors in this section of the circuit are mounted immediately beneath the amplifier.

(d) The unit must be powered continuously, except for disconnections lasting only a few seconds, in order to avoid thermal fluctuations in the instrument case.

(e) Several controls are mounted on the outer instrument case, including the following :

  (i) A switch selecting the bandwidth of the amplifier, capable of increasing the response of the system by a factor of ten. Usually, the lower response is used, to minimise the effects of any electrical interference.

(ii) Several potentiometers which introduce an offset voltage (after the initial amplification, in order to minimise the amount of electrical noise which may be introduced by this circuit). This offset voltage is used to remove the initial voltage Vo in order to facilitate recording of the ΔV signal.

(iii) Access to a trimming potentiometer, in the internal case, to zero the amplifier.

(f) The amplifier output is displayed, to five significant figures on a digital voltmeter, and on a chart recorder.

(g) In practice, the electrical noise on the signal, when a CT specimen is connected and ready for testing, is approximately 0.2 μV peak-to-peak.

APPENDIX E

MECHANICAL TESTING SYSTEM MODIFICATIONS

The extremely low voltages measured in P.D. systems may be completely masked by electrical noise from earth loops. In particular, the considerable currents which can circulate in a testing machine frame can produce electrical signals in the moving parts of the system (including the specimen). It is therefore necessary to ensure that the specimen is completely insulated from the testing machine. For compression testing rigs, this is relatively simple, a layer of insulating material (in this case, 12.5 mm thick "Tufnol") being inserted beneath the loading platens. Such materials, however, usually have low tensile strength, and tension rig insulators must use a tension/compression load transfer system such as that shown in Fig. E1. This arrangement, using high-strength steel bolts with insulating inserts, can accommodate loads in excess of 300 kN, and two such systems are of course necessary for full insulation.

An alternative approach involves using insulating sleeves around the loading pins. This simple system is effective at low loads, but the uneven distribution of load along the pin may lead to sleeve failure at high loads.

Further insulation is required on all metal surfaces which contact the specimen faces, in order to avoid providing alternative current paths between the current input leads, and glass insulating tape was found to have suitable abrasion resistance for this purpose.

In all other respects, the testing system is unchanged.

APPENDIX F

POTENTIAL CALIBRATION SYSTEM AND RESULTS

F.1 Experimental

Calibrations are performed using two-dimensional analogue specimens cut from conducting paper. Aluminised card and graphitised paper have been used, the latter having higher resistance and hence producing higher voltages, which lead to more accurate calibration data. Analogue specimens are cut from sheets of paper, with as large a magnification as possible in order to obtain increased accuracy in determining the dimensions of the crack, and current is introduced by attaching the uninsulated current lead to the paper with staples. Potential probes are connected in the same way, and the circuit used is shown in Fig. F1. As "constant" current power supplies are often unreliable at the low current levels required for conducting paper specimens, a resistor and voltmeter system is used to monitor changes in the current during the calibration procedure, and corrections are made to the voltage data when such variations occur.

The calibration closely parallels the real test; after noting Vo, a "crack" is cut in the specimen and, taking care to insulate the cut edges of the crack, the value of V is recorded. This is continued until the crack extends some way beyond the maximum crack length required in the real specimen geometry.

Calibrations have been performed on various specimen geometries, some of which are illustrated in Fig. F2.

F.2 Equipotential Determination

When a new specimen design is being considered, it is necessary to determine the best positions for current input leads and potential probes. Ideally, the probe position should be chosen to give maximum response to crack length changes whilst minimising the sensitivity of the calibration to minor variations in probe location. This latter condition is satisfied if probes are positioned in regions where the potential gradient is low.

Analogue specimens may be used to determine the potential distribution in each geometry; the current is connected in the usual way, and a voltmeter is used to locate points on the specimen surface which have equal potentials relative to any convenient fixed point in the circuit. By plotting equipotentials at, say, 0.5 volt intervals, regions with low potential gradients may be readily identified as having widely-spaced equipotential lines. As an example, it was necessary to choose probe positions for the J2543 geometry (similar to the J2503 specimen shown in Fig. F2); equipotentials determined by the above method are shown in Fig. F3, and it is clear that the displacement measuring points marked A are suitable potential measurement positions.

Equipotential plotting may also be used to determine the effect of changes in geometry upon the current distribution in the specimen [16].

F.3 Potential Calibration Polynomials

In order to use the calibration data in computer processing of the test results it is desirable that a curve be fitted to the data points, and the form of the curve chosen is a polynomial in either (V/Vo) or (ΔV/Vo).

A least-squares fit was found to be satisfactory in most cases, in that the curve fitted the experimental data well. However it is essential to avoid curve-fitting fluctuations in the regions between the data points. Such fluctuations, resulting from the use of very high-order curve fitting, may produce errors later in the data-processing sequence, when the crack length and number of cycles relationship is differentiated to derive crack growth rates. Any high-order fluctuations in the calibration equation would lead to significant errors in crack growth rate, and a set of test data was processed using increasing orders of polynomial in an attempt to detect any such errors. No signs of scatter in growth rate were encountered using orders up to six, and hence the high accuracy of sixth-order polynomials was chosen for most calibrations.

Calibration equations for CTS, beam and ring specimen geometries are given in Table I.

APPENDIX G

COMPUTER PROCESSING OF TEST RESULTS

A considerable amount of data is generated by each test, consisting of ΔV and maximum and minimum load values noted at intervals of approximately 1000 cycles. Computer handling of this data is necessary and all tests are placed in computer file 'DATA' which is subsequently read by the FORTRAN program 'PDPROG'.

After the parameters describing the specimen geometry, material properties and test variables (such as Vo) have been placed on file, the bulk of the data is read in using the format -

$$N_1 \; ; \; V_1 \; ; \; L_{max_1} \; ; \; L_{min_1}$$

$$N_2 \; ; \; V_2$$

$$N_3 \; ; \; V_3$$

with new values of L_{max} and L_{min} being inserted only when necessary.

The main program 'PDPROG' which operates as shown in Fig. G1, reads this data, and, selecting the correct P.D. calibration polynomial, derives a crack length value for each data point. Crack length values and load data are then used in the appropriate stress-intensity calibration equation to derive values of K_{max} and ΔK for each data point.

In order to calculate crack growth rates accurately it is necessary to consider only a limited number of data points. However, simply using the crack length increment between two data points will introduce unacceptable scatter in the growth rate estimates, and the approach used is to least-squares fit a quadratic expression to seven consecutive pairs of a and N values, and to differentiate at the central point. The program then moves along by one reading and the process is repeated. The output from the program includes plotted curves of $log(da/dN)$ vs. $log(\Delta K)$, a vs. N, $log(da/dN)$ vs. a, and $log(\Delta K)$ vs. a.

A copy of 'PDPROG' is available from MRL.

TABLE I

CALIBRATION EQUATIONS FOR POTENTIAL DROP CRACK MONITORING IN COMPACT TENSION, BEAM AND RING SPECIMEN GEOMETRIES

$$\frac{a}{W} = \sum_{0}^{6} A_n \left(\frac{\Delta V}{Vo}\right)^n \quad \text{or} \quad \sum_{0}^{6} B_n \left(\frac{V}{Vo}\right)^n$$

	CTS $\left(\frac{a_o}{W} = 0.3\right)$	Ring $(R_i/R_o = 0.5)$
A_o	0.304266	0.07202
A_1	0.978659	2.14632
A_2	- 1.49606	- 4.61995
A_3	4.89826	8.40463
A_4	- 9.86845	- 8.94370
A_5	9.40817	4.83124
A_6	- 3.39216	- 1.03089
Range of $\frac{a}{W}$	$0.3 < \frac{a}{W} < 0.82$	$0.1 < \frac{a}{W} < 0.94$

	Beam $(a_o/W = 0.25)$(45° V-notch)
B_o	- 0.684657
B_1	1.872426
B_2	- 1.487903
B_3	0.703605
B_4	- 0.169617
B_5	0.0161446
B_6	0
Range of $\frac{a}{W}$	$0.25 < \frac{a}{W} < 0.7$

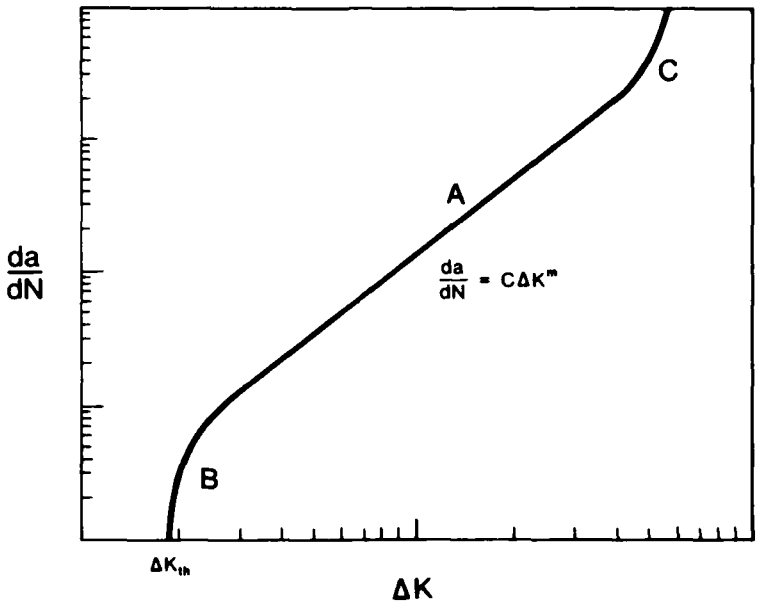

FIG. 1 - The linear relationship between crack growth rate and the crack tip stress intensity range (ΔK) in Region A, shown schematically. At low stress-intensities, growth rate decreases rapidly to zero. In Region C, additional fracture modes occur and result in increased crack growth rates.

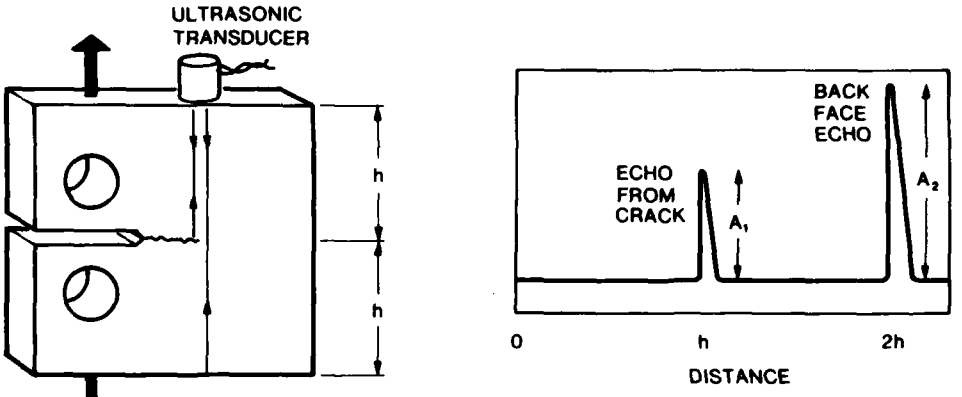

(a) (b)

FIG. 2 - (a) One method of ultrasonic crack monitoring; the transducer is moved along the upper surface of the test specimen in such a manner that the responses shown in (b) from the crack and from the lower face are maintained in the same ratio (A_1/A_2). The ultrasonic probe then moves at the same rate as the crack tip.

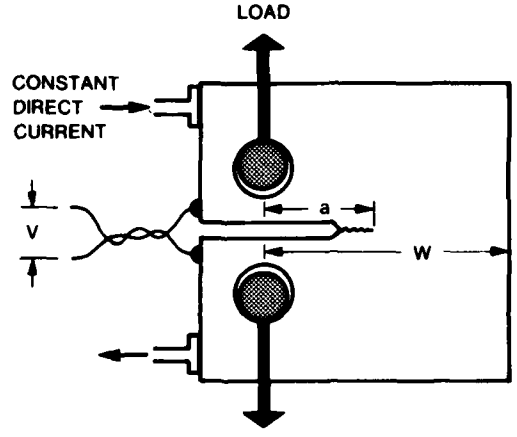

(a)

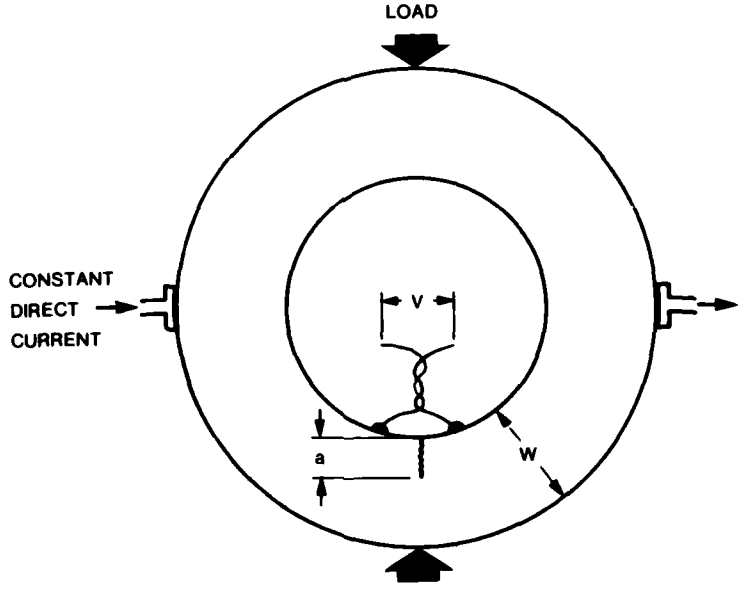

(b)

FIG. 3 - Arrangement of current input leads and potential probe leads for potential drop crack length determination in (a) a compact tension specimen (CTS) and (b) in a ring specimen loaded in compression across a diameter.

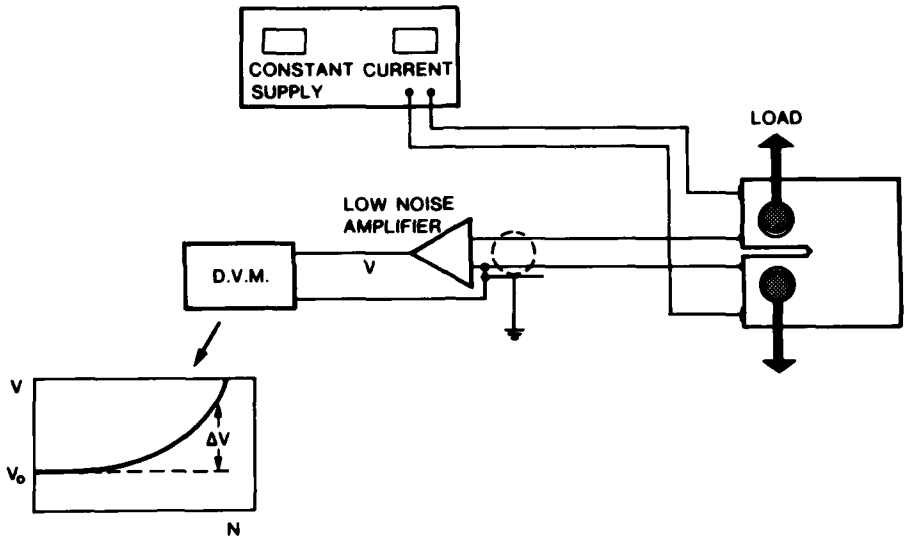

FIG. 4 - Schematic representation of the P.D. system used on a compact tension specimen. The amplifier output V increases from the initial (no crack) value Vo.

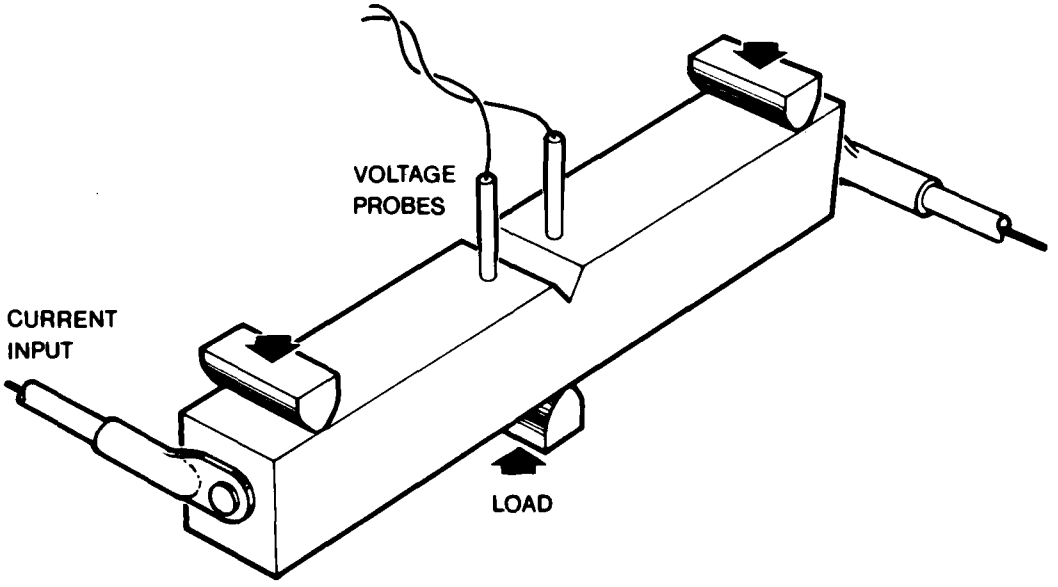

FIG. 5 - Current input lead and potential probe positions for a beam specimen containing a V-notch. The current input lead position on the end of the specimen is not critical in this geometry.

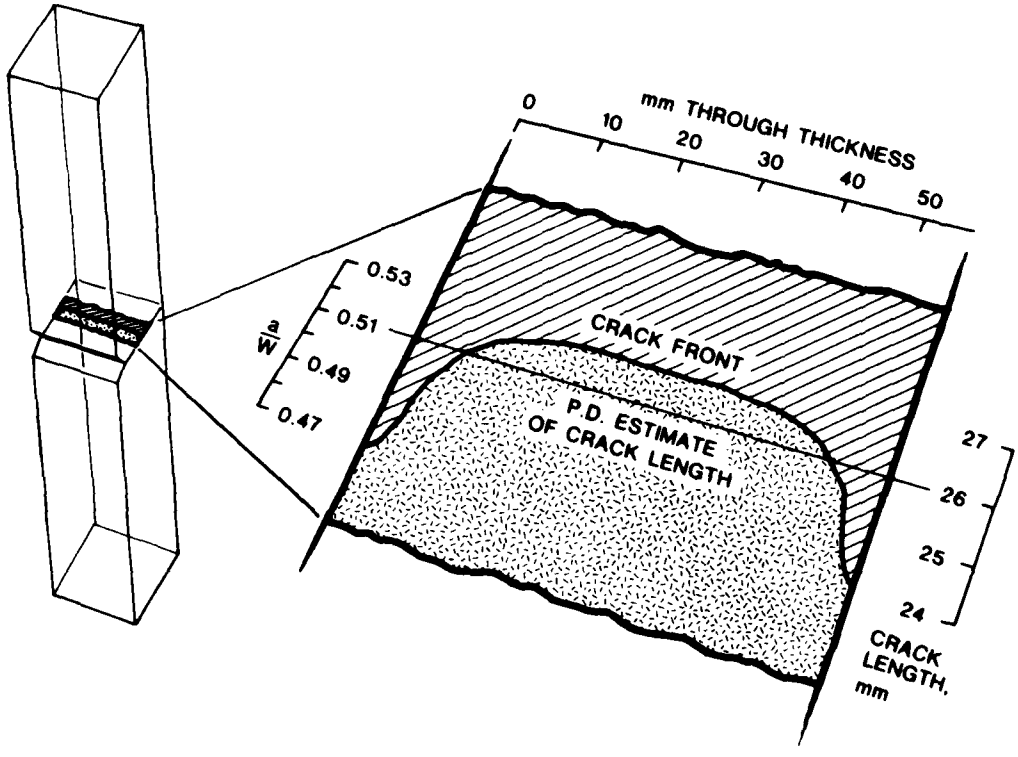

FIG. 6 - Crack front profile (with the crack growing in the plane of the paper) in a 57 mm thick beam specimen with W = 51 mm. The crack length indicated by the P.D. system is marked, as are the crack lengths measured on the two sides of the specimen.

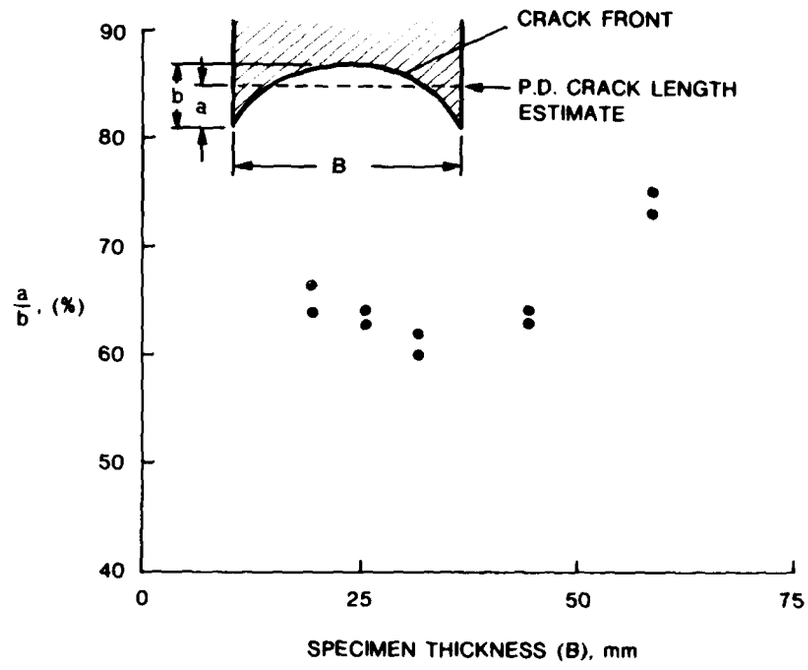

FIG. 7 - Variation in P.D. crack length estimate (expressed as a percentage of the distance between the 'trailing' and 'leading' crack front positions) as the specimen thickness increases. Specimens are mild steel beams; in all thicknesses, the P.D. system provides an 'average' length of crack. In the thickest specimen, where the crack has a straight central portion, the P.D. estimate naturally approaches the 'leading' edge of the crack more closely than in thinner specimens.

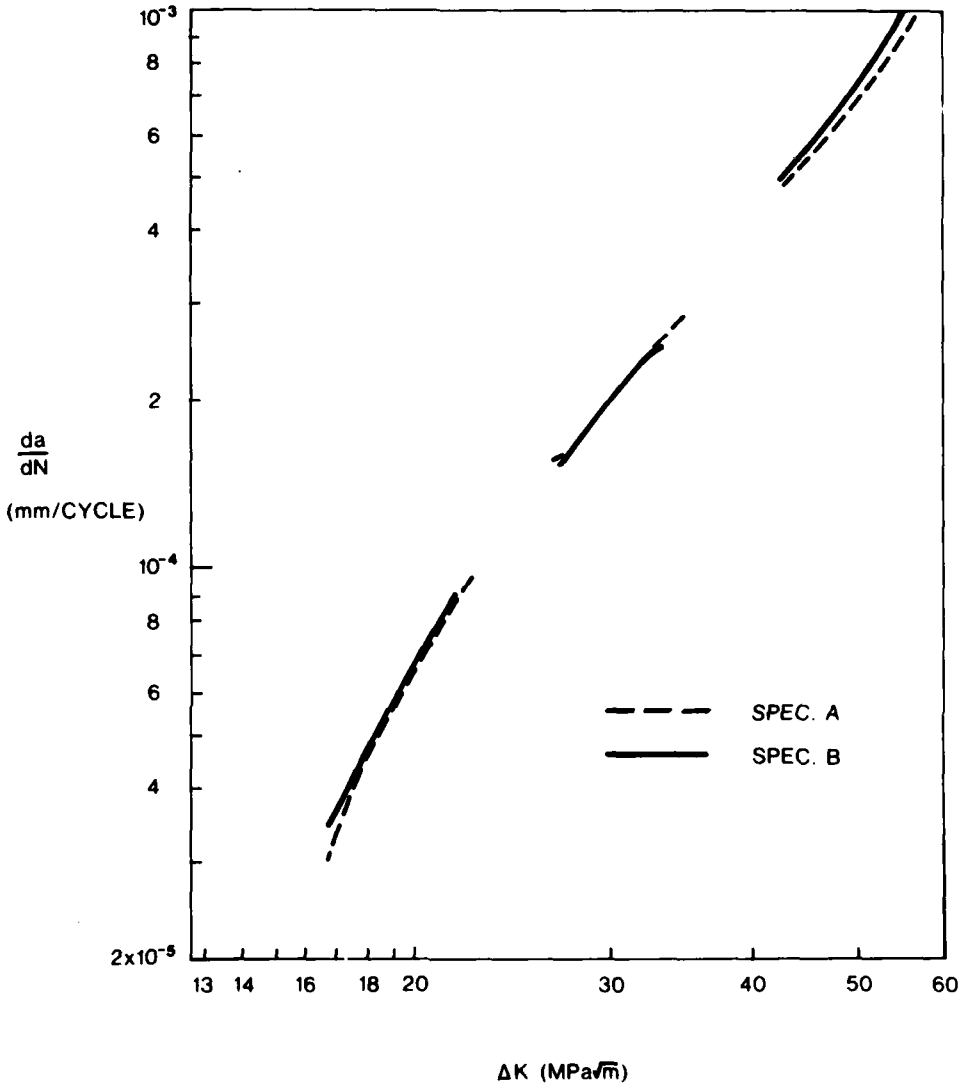

FIG. 8 - Crack growth rate and ΔK data for two identical specimens of an ESR steel. Crack growth rates agree very closely, in the high- ΔK region, where local material variations are expected to have a significant effect.

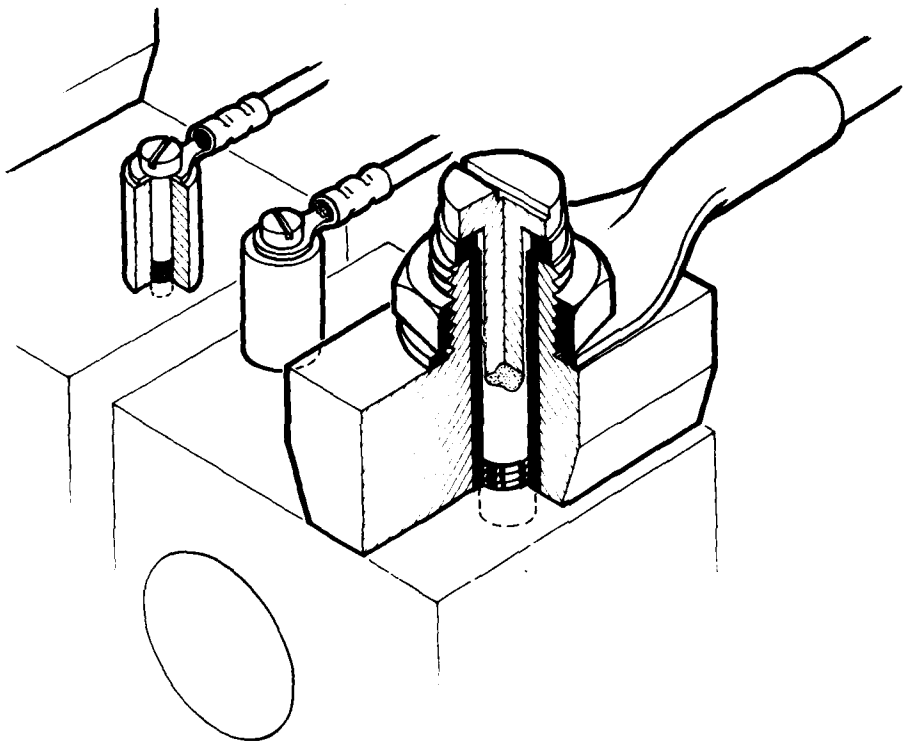

FIG. B1 - Current input lead and potential probe configuration for the CT specimen geometry. The current lead attaching screw carries no current, and steel screws are used for the potential probes, to minimise thermal potentials.

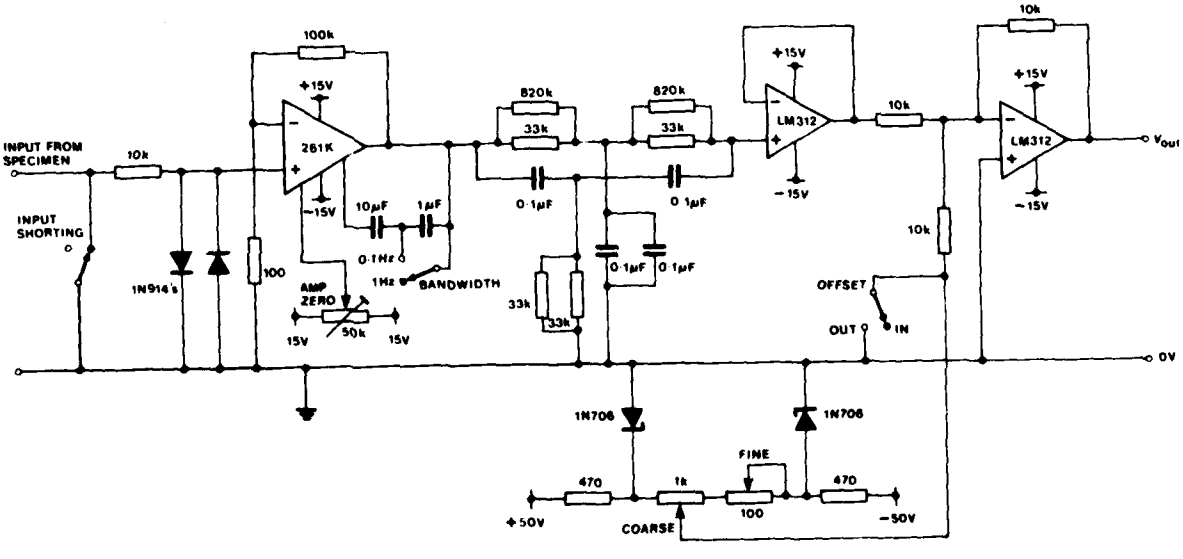

FIG. D1 - Circuit diagram of P.D. amplifier system.

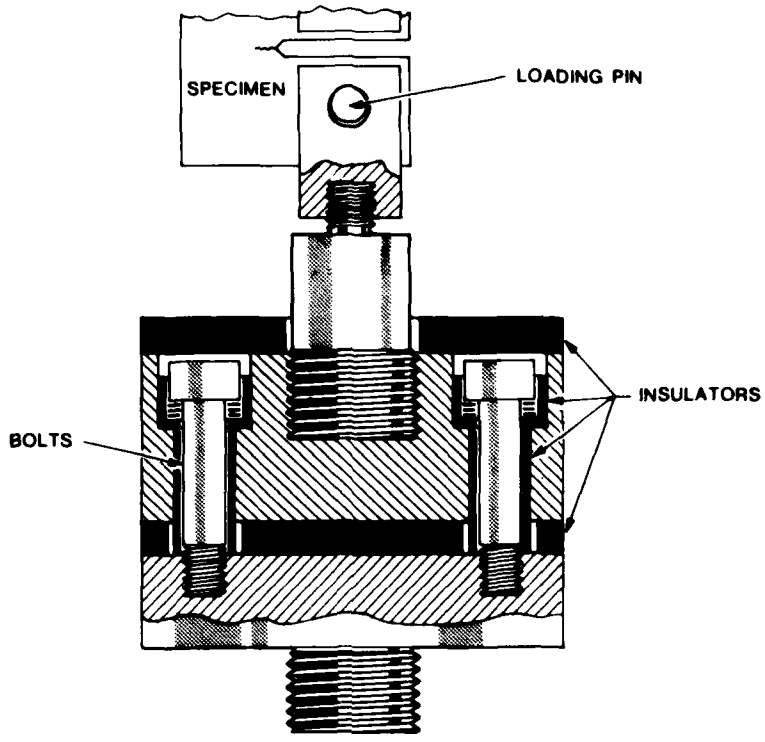

FIG. E1 - Tension testing rig insulation system. High tensile-strength bolts are used to transfer the load.

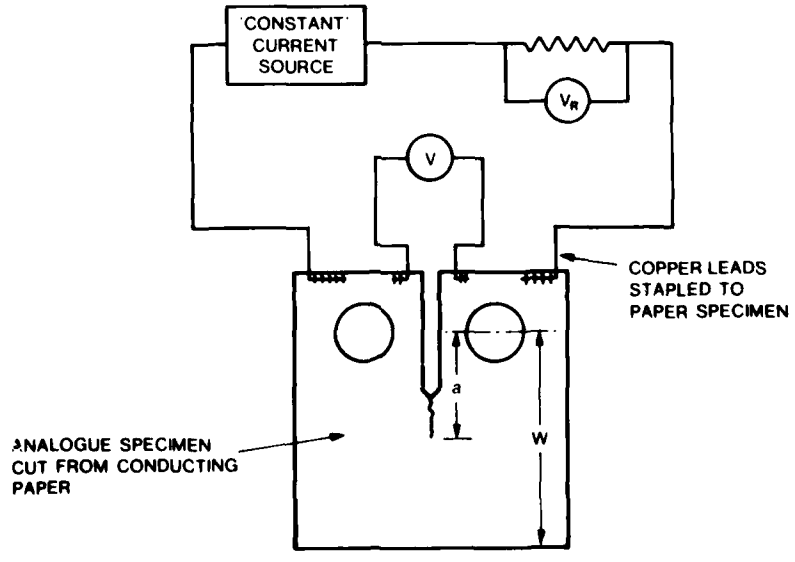

FIG. F1 - Circuit used for calibrating the CT specimen geometry. V_R is used to monitor changes in current.

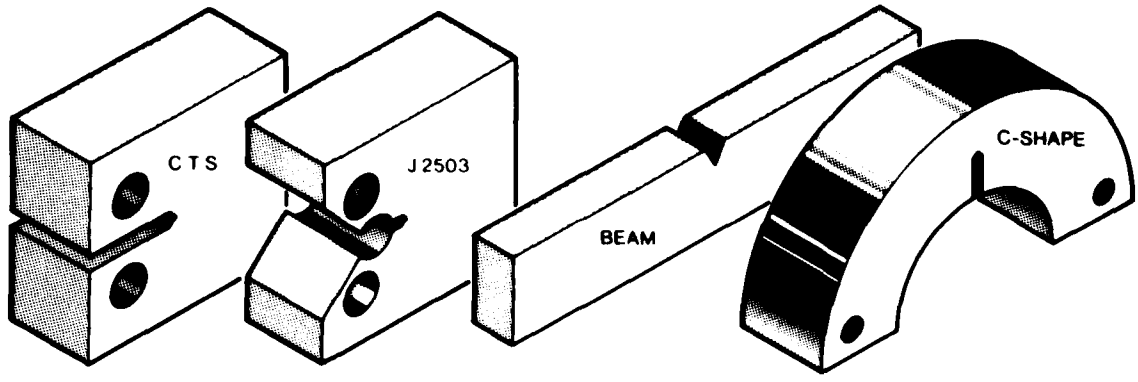

FIG. F2 - Various geometries for which calibrations have been performed.

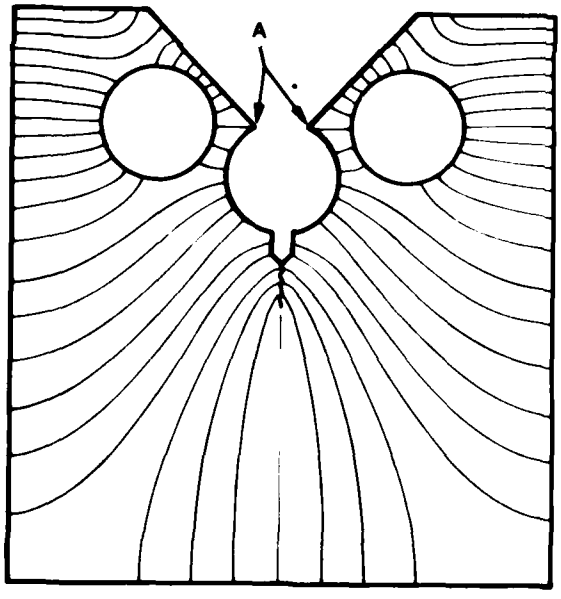

FIG. F3 - Equipotential lines in the J2543 specimen. The wide spacing of the lines near positions A indicates that the calibration will not be greatly affected by errors in probe location in this region. Current flow lines are normal to the equipotentials.

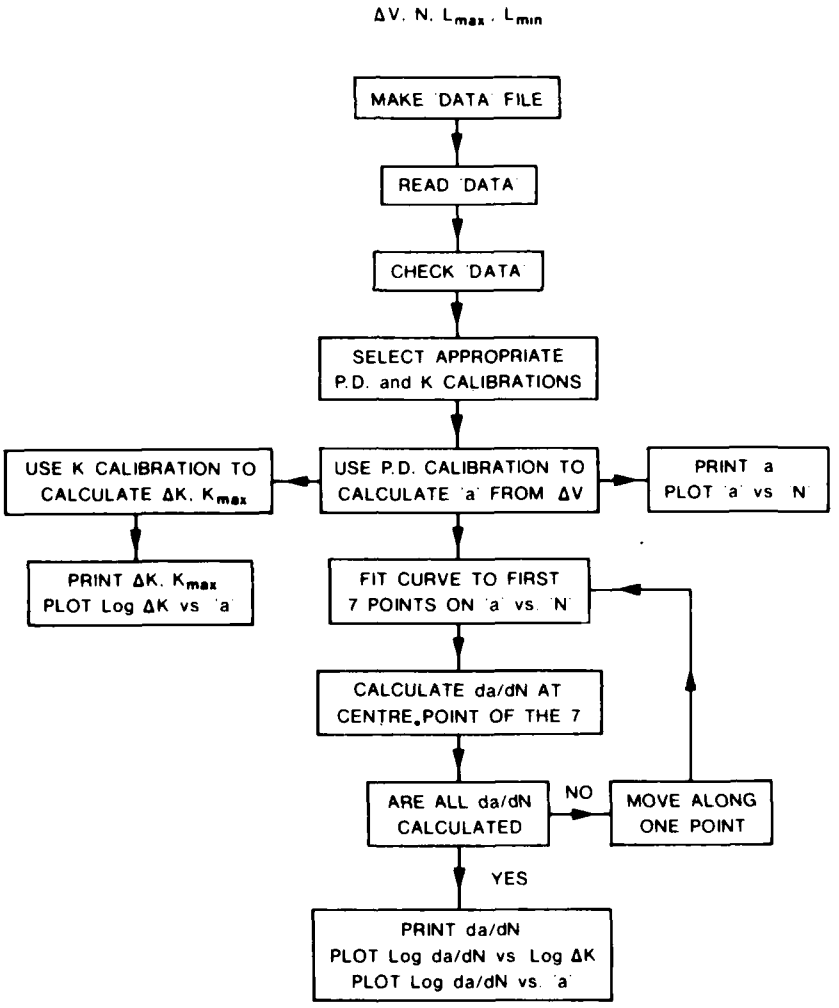

FIG. G1 - Flow chart of programs 'DATA' and 'PDPROG'.

(MRL-R-755)

DISTRIBUTION LIST

MATERIALS RESEARCH LABORATORIES

Chief Superintendent
Superintendent, Metallurgy Division
Dr. M.E. de Morton
Dr. G. Clark
Library
Librarian, Materials Testing Laboratories, N.S.W. Branch
(Through Officer-in-Charge)

DEPARTMENT OF DEFENCE

Chief Defence Scientist
Deputy Chief Defence Scientist
Controller, Projects and Analytical Studies
Superintendent, Science and Technology Programmes
Scientific Adviser - Army
Air Force Scientific Adviser
Navy Scientific Adviser
Chief Superintendent, Aeronautical Research Laboratories
Director, Defence Research Centre
Senior Librarian, Defence Research Centre
Librarian, R.A.N. Research Laboratory
Officer-in-Charge, Document Exchange Centre (16 copies)
Technical Reports Centre, Defence Central Library
Central Office, Directorate of Quality Assurance - Air Force
Deputy Director Scientific and Technical Intelligence,
Joint Intelligence Organisation
Head, Engineering Development Establishment
Librarian, Bridges Library, Royal Military College

DEPARTMENT OF PRODUCTIVITY

NASA Canberra Office
Head, B.D.R.S.S. (Aust.)

OTHER FEDERAL AND STATE DEPARTMENTS AND INSTRUMENTALITIES

The Chief Librarian, Central Library, CSIRO
Australian Atomic Energy Commission Research Establishment

DISTRIBUTION LIST

(Continued)

MISCELLANEOUS - OVERSEAS

Defence Scientific and Technical Representative, Australian High Commission, London, England
Assistant Director/Armour and Materials, Military Vehicles and Engineering Establishment, Surrey, England
Reports Centre, Directorate of Materials Aviation, Kent, England
Library - Exchange Desk, National Bureau of Standards, Washington, U.S.A.
U.S. Army Standardization Representative, Canberra, A.C.T.
The Director, Defence Scientific Information and Documentation Centre, Delhi, India
Colonel B.C. Joshi, Military, Naval and Air Adviser, High Commission of India, Red Hill, A.C.T.
Director, Defence Research Centre, Kuala Lumpur, Malaysia
Exchange Section, British Library, Lending Division, Yorkshire, England
Periodicals Recording Section, Science Reference Library, British Library, Holborn Branch, London, England
Library, Chemical Abstracts Service, Columbus, Ohio, U.S.A.
INSPEC: Acquisition Section, Institution of Electrical Engineers, Herts, England
Overseas Reports Section, Defence Research Information Centre, Kent, England
Engineering Societies Library, New York, U.S.A.